Chemical Science

EDGE ARTICLE

View Article Online
View Journal | View Issue

Check for updates

Cite this: *Chem. Sci.*, 2018, **9**, 4493

Isolable iodosylarene and iodoxyarene adducts of Co and their O-atom transfer and C–H activation reactivity†

Ethan A. Hill, Margaret L. Kelty, Alexander S. Filatov and John S. Anderson *

Received 13th March 2018
Accepted 19th April 2018

DOI: 10.1039/c8sc01167b

rsc.li/chemical-science

We report an unusual series of discrete iodosyl- and iodoxyarene adducts of Co. The formation of these adducts was confirmed by a suite of techniques including single crystal X-ray diffraction. The reactivity of these adducts with O-atom acceptors and an H-atom donor has been investigated with particular focus on elucidating mechanistic details. Detailed kinetic analysis allows for discrimination between proposed oxo and adduct mediated mechanisms. In particular, these reactions have been interrogated by competition experiments with isotopically labelled mixtures which shows that all of the studied adducts display a large KIE. These studies suggest different mechanisms may be relevant depending on subtle substituent changes in the adduct complexes. Reactivity data are consistent with the involvement of a transient oxo complex in one case, while the two other systems appear to react with substrates directly as iodosyl- or iodoxyarene adducts. These results support that reactivity typically ascribed to metal-oxo complexes, such as O-atom transfer and C–H activation, can also be mediated by discrete transition metal iodosyl- or iodoxyarene adducts that are frequent intermediates in the generation of oxo complexes. The influence of additional Lewis acids such as Sc^{3+} on the reactivity of these systems has also been investigated.

Open Access Article. Published on 23 April 2018. Downloaded on 2/20/2026 3:42:12 PM.
This article is licensed under a Creative Commons Attribution-NonCommercial 3.0 Unported Licence.

Introduction

Iodosylbenzene (PhIO) and its derivative iodosylarenes have been widely used as O-atom donor reagents in transition metal mediated oxidation reactions including C–H hydroxylation and O-atom transfer to substrates.[1–4] The mechanisms of these reactions are proposed to proceed *via* the formation of a metal iodosylarene adduct followed by transfer of an oxygen atom with concomitant oxidation of the metal center to form iodoarene and a high-valent metal-oxo complex as the active oxidant.[5–11] Concurrent to the development of this mechanistic paradigm have been studies suggesting that hypervalent iodine adducts themselves are likewise capable of performing atom transfer reactions to substrates.[12–24] This alternative mode of activity has motivated efforts at isolating discrete transition metal iodosylarene adducts and studying their reactivity. While rare, there are some examples of well characterized transition metal iodosylarene adducts, including several that have been structurally characterized.[25–31] Much of the focus thus far has been on Fe and Mn adducts, as these metals are most frequently featured in oxidation catalysis. More recently, iodosylarenes have been used to generate high-valent Co complexes as well.[32–34] Iodosylarene adducts have been cited in these studies as intermediates, but have not yet been isolated or thoroughly characterized to examine their reactivity.

Herein, we report the first isolable examples of Co iodosyl- and iodoxyarene adducts $[Co(II)Tp^{Ad,Me}(^{s}PhIO)]^{+}$ (**1**), $[Co(II)Tp^{tBu}(^{s}PhIO)]^{+}$ (**2**), and $[Co(II)Tp^{tBu}(^{s}PhIO_2)]^{+}$ (**3**) (Tp = hydrotris(pyrazolyl)borate and ^{s}Ph = 2-(*tert*-butylsulfonyl)phenyl; Scheme 1). Complexes **1**, **2**, and **3** have been crystallographically characterized and detailed kinetic studies reveal a range of reactivity for these three adducts. Complex **1** shows unique behavior that may be consistent with transient oxo formation, but complexes **2** and **3** appear to react as adducts. The observed C–H activation kinetic isotope effect (KIE) is large in all cases, potentially consistent with proton tunnelling transition

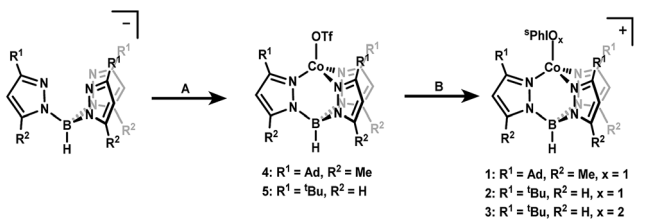

Scheme 1 Synthetic routes to generate complexes **1**–**5** starting from the appropriate Tp ligand. (A) $Co(MeCN)_6(OTf)_2$, DCM, N_2, r.t., (B) (1) 1.1 equivalents $NaBAr^{F}_4$ (2) 1.1 equivalents $^{s}PhIO_x$, Et_2O, N_2, r.t.

Department of Chemistry, The University of Chicago, 5735 S. Ellis Ave, Chicago, IL 60637, USA. E-mail: jsanderson@uchicago.edu

† Electronic supplementary information (ESI) available. CCDC 1818929–1818931 and 1818933–1818935. For ESI and crystallographic data in CIF or other electronic format see DOI: 10.1039/c8sc01167b

Open Access Article. Published on 23 April 2018. Downloaded on 2/20/2026 3:42:12 PM.
This article is licensed under a Creative Commons Attribution-NonCommercial 3.0 Unported Licence.

states.[35–38] These observations, in addition to controls with redox-innocent Lewis acids, suggest that Lewis acid activation of iodosylarenes leads to H-atom abstraction with large KIEs.

Results and discussion

Synthesis of adduct complexes

Starting materials and ligands were synthesized according to previously reported procedures with slight modifications in some cases (see ESI†).[39–45] Treatment of the previously reported $NaTp^{Ad,Me}$ or KTp^{tBu} ligands with $Co(MeCN)_6(OTf)_2$ in dichloromethane (DCM) yielded complexes [Co(II)$Tp^{Ad,Me}$(OTf)] (**4**) and [Co(II)Tp^{tBu}(OTf)] (**5**) (OTf = trifluoromethanesulfonate) in 76% and 64% yield as bright blue crystalline solids. The ^{1}H NMR spectra of these complexes confirm overall C_3-symmetry in solution with shifted resonances characteristic of paramagnetic species. The ^{19}F NMR spectra of **4** and **5** support the coordination of OTf in solution as demonstrated by a shift of the $-CF_3$ resonance to −8.7 and −30.0 ppm, respectively (the signal from free OTf appears at −78 ppm). Additionally, the EPR spectra of **4** and **5** are consistent with an expected $S = 3/2$ spin state for high-spin Co(II) centers (see ESI†). Both **4** and **5** display similar electrochemistry, with irreversible oxidations at ∼2 V *vs.* $[FeCp_2]^{0/+}$ (see ESI†).

Synthesis of the cobalt iodosylarene adducts was carried out by treatment of **4** and **5** with 1.1 equivalents of ^{s}PhIO and $NaBAr^F_4$ (BAr^F_4 = tetrakis(3,5-bis(trifluoromethyl)phenyl)borate) in diethyl ether (Et_2O). This procedure resulted in the clean formation of new paramagnetic species that maintain C_3-symmetry in solution as judged by ^{1}H NMR. A new set of paramagnetically shifted signals consistent with a bound ^{s}PhIO ligand are also observed, which suggests the formation of a stable adduct in solution (see ESI†). These species were assigned as the cationic iodosylarene adducts **1** and **2** that can be isolated as blue powders in 76% and 83% yield, respectively (Scheme 1). Complex **3** was first observed as a by-product in ^{1}H NMR spectra from the synthesis of **2**. The identity of **3** as an ^{s}PhIO$_2$ adduct was suspected due to literature reports that upon standing in solution, ^{s}PhIO will disproportionate into ^{s}PhI and ^{s}PhIO$_2$.[41] Treatment of **5** with independently prepared ^{s}PhIO$_2$ in the presence of $NaBAr^F_4$ in Et_2O led to the isolation of the targeted ^{s}PhIO$_2$ adduct **3** in 67% yield as a light blue powder. Solution ^{1}H NMR spectra showed that complex **3** retains overall C_3-symmetry with paramagnetically shifted resonances. The X-band EPR spectra of complexes **1–3** are consistent with $S = 3/2$ Co(II) centers.

Crystallography

Single crystals of **4** and **5** were grown from concentrated solutions in Et_2O layered with petroleum ether and stored at −35 °C for a few days. The X-ray diffraction (XRD) structures of **4** and **5** confirm coordination of the Tp ligand and OTf counter-ion to the Co center (see ESI†). The Co centers of these complexes adopt the expected pseudo-tetrahedral geometry observed for other reported [CoTpX] complexes.[46–51] One metric to note is the deviation of the B–Co–O angle from nearly linear in **5** (175.59(4)°) to 161.11(5)° in **4**. This distortion is attributed to the steric clashing of the $-CF_3$ group with the adamantyl substituents that is not present for the *t*-butyl substituted Tp ligand.

Crystals of **1** were grown under the same conditions to those of **4** and **5**, while crystals of **2** were grown from a concentrated solution of Et_2O layered with hexamethyldisiloxane and stored at −35 °C for 7 days. The XRD structures of **1** and **2** confirm the expected pseudo-tetrahedral geometry at Co and furthermore confirm coordination of the ^{s}PhIO ligand in the solid state (Chart 1). The average Co–N bond distances are nearly identical to those in **4** and **5**, suggesting the oxidation and spin state of Co is unchanged, which is also corroborated by the aforementioned spectroscopic data. The I–O bond lengths in **1** and **2** are 1.878(6) and 1.891(3) Å. When compared to the I–O distance of 1.848(5) Å for free ^{s}PhIO there appears to be minimal activation of the iodosylarene by the Co center in these complexes.[39] The Co–O bond lengths are 1.920(6) and 1.934(3) Å, which are comparable with other Co(II)–O bonds as well as the OTf starting complexes **4** and **5**.[52] Complex **3** has also been structurally characterized with crystals grown from a layered Et_2O/petroleum ether solution stored at −35 °C. The average Co–N bond lengths of **3** are nearly identical to those of the starting Co–OTf complex **5** and the I–O bond lengths of 1.814(3) and 1.780(3) Å are also similar to those in the structure of free ^{s}PhIO$_2$ at 1.822(3) and 1.796(2) Å.[41] Isolable iodoxyarene adducts are quite rare, and to our knowledge **3** represents the first structurally characterized example with a transition metal.[30] While the I–O bond lengths in this series of complexes are all similar to those reported in the free hypervalent iodine reagents, suggestive of minimal activation, the S=O···I interactions show more sensitivity to Co coordination. The S=O···I distances are in fact shorter than those found in the structures of the free oxidants, suggesting some effect of binding the Lewis acidic Co(II) center. For **1** and **2** the distances have substantially shortened to 2.481(6) and 2.520(3) Å compared to 2.707(5) Å for free ^{s}PhIO.[39] For **3**, an analogous but smaller contraction from 2.693(2) Å to 2.662(3) Å is observed.[41] In the case of **3**, there is an unusual close interaction between a solvent THF molecule and the iodine center which may also speak to a more electron deficient adduct (see ESI†).[30]

The structural data for **1**, **2**, and **3** support the formation of well-defined adducts with no substantial change in the Co oxidation state, spin state, or activation of the hypervalent iodine unit. This series of complexes represents an unusual family of isolable, well-characterized hypervalent iodine adducts. These species are generally rare and, as mentioned in the introduction, there have been no examples to date of isolated Co adducts despite the use of iodosylarene reagents in Co-mediated oxidation reactivity.[32–34]

Reactivity studies

The isolability of this series of iodosyl- and iodoxyarene adducts prompted us to investigate their oxidative activity. We were particularly interested in examining the O-atom transfer and C–H activation reactivity of these complexes with a focus on developing an understanding of the mechanism of these

 This journal is © The Royal Society of Chemistry 2018

Open Access Article. Published on 23 April 2018. Downloaded on 2/20/2026 3:42:12 PM.
This article is licensed under a Creative Commons Attribution-NonCommercial 3.0 Unported Licence.

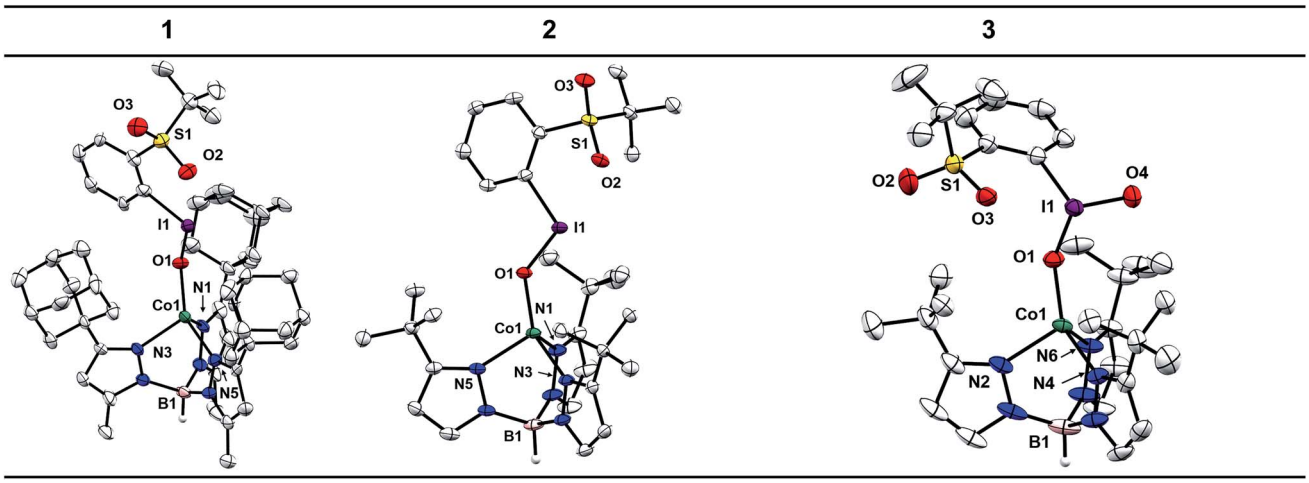

Chart 1 XRD structures and selected bond lengths for complexes **1**, **2**, and **3** (Å). Structures depicted as ellipsoids at 50% probability. Hydrogen atoms (other than B–H), BAr^F_4 counter ions, and solvent molecules omitted for clarity.

transformations. More specifically, we wanted to determine whether high-valent oxo complexes were generated over the course of these reactions or whether the adducts themselves could mediate oxidative reactivity.

While complexes **1**, **2**, and **3** were stable enough to allow for their isolation, they do slowly decompose in solution at room temperature. Complex **1** decays with a rate constant of $k_{obs} = 1.4(\pm0.4) \times 10^{-5}$ s^{-1} at room temperature in Et_2O (Fig. 1, Table 1). Analysis of the resulting reaction mixture by ^{1}H NMR spectroscopy indicated a complex array of peaks that were not easily assigned (see ESI†). Analysis by ESI-MS shows evidence of incorporation of oxygen into the ligand backbone suggesting ligand-based oxidation as a mode of decay for complex **1** (see ESI†). Attempts to react **1** with external substrates were carried out by addition of either 10 equivalents of thioanisole or up to 100 equivalents of 9,10-dihydroanthracene (DHA). In both cases no increase in the rate of decay was observed by UV-vis spectroscopy (see ESI†). Complex **1** does react rapidly with PMe_3 in ~120 s to generate what is assigned as an $OPMe_3$ adduct. The assignment of the phosphine oxide adduct is supported by independent synthesis from $OPMe_3$ (see ESI†).

Complexes **2** and **3** were similarly unstable in solution and decayed with markedly slower rate constants than **1**. The decay of **2** was monitored *via* UV-vis spectroscopy to obtain a rate of decay with $k_{obs} = 6.3(\pm0.8) \times 10^{-7}$ s^{-1} at room temperature in Et_2O. Complex **3** decayed with $k_{obs} = 6.3(\pm0.4) \times 10^{-6}$ s^{-1} as monitored with ^{1}H NMR spectroscopy at room temperature in $CDCl_3$. In addition, the decay profiles of both complexes are much less complicated than that observed for **1**; complex **2** decays to a single paramagnetic product and **3** decays to this same product while also producing some amount of **2** (see ESI†). Similar to **1**, these species show rapid reactivity with phosphines to generate putative phosphine-oxide adducts (also supported by independent syntheses, see ESI†). Unlike **1**, both **2** and **3** show distinct reactivity with other substrates. In the presence of 10 equivalents of thioanisole, the rate of disappearance of **2** or **3** increased by roughly two-fold. In the reactions of **2** and **3** with thioanisole, the adduct of the corresponding oxidized substrate, phenylmethylsulfoxide, was observed by ^{1}H NMR spectroscopy. This assignment was again confirmed by independent synthesis of the adduct (see ESI†). Smaller, concentration dependent rate enhancements were observed for **2** and **3** treated with excess DHA ($k_2 = 2.4 \times 10^{-6}$ and 1.4×10^{-5} M^{-1} s^{-1}, Fig. 2 and ESI†). In this case,

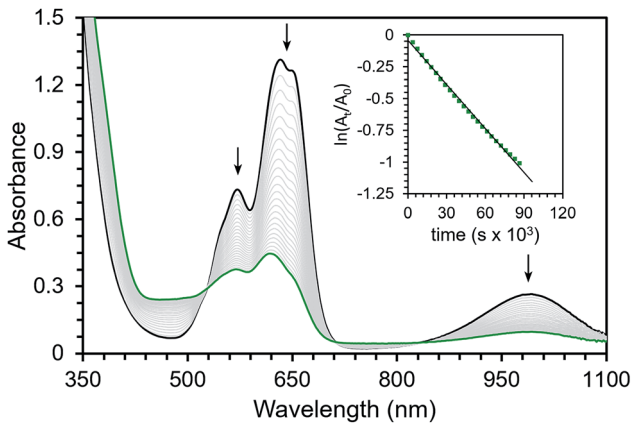

Fig. 1 UV-vis spectral changes during the decay of **1** (black, 2.5 mM) in Et_2O at 23 °C over 24 h. Inset shows plot of the natural log of the change in concentration of **1** (monitored at 995 nm) *vs.* time with linear fit ($R^2 = 0.98$).

Table 1 Observed reaction rates and KIEs of **1**, **2**, and **3**[a]

Substrate	**1**[b]	**2**[b]	**3**[c]
Self-decay	14(4)	0.63(8)	6.3(4)
Thioanisole	No change	1.12(9)	16(8)
9,10-DHA	No change	1.2(3)	10.3(2)
9,10-DHA KIE[d]	>12	14(5)	9(1)

[a] Reported rates are 10^{-6} s^{-1}. Reaction conditions: 2.5 mM cobalt complex, 23 °C, 25 mM substrate (250 mM for DHA). [b] Monitored *via* UV-vis spectroscopy in Et_2O. [c] Monitored *via* ^{1}H NMR spectroscopy in $CDCl_3$. [d] 1 : 1 mixture of 125 mM each H_4-DHA and D_4-DHA in DCM.

Open Access Article. Published on 23 April 2018. Downloaded on 2/20/2026 3:42:12 PM.
This article is licensed under a Creative Commons Attribution-NonCommercial 3.0 Unported Licence.

anthracene was detected by GCMS analysis of the reaction mixtures (see ESI†).

Control reactions were also performed to assess the relative reactivity of **1** and **2** compared to free ^{s}PhIO. The complementary study to compare **3** with $^{s}PhIO_2$ was hindered by the extremely poor solubility of $^{s}PhIO_2$ in organic solvents. The rate of decay of ^{s}PhIO monitored *via* ^{1}H NMR spectroscopy with either 50 equivalents of DHA or 10 equivalents of thioanisole gave rates of $1.7(\pm0.2) \times 10^{-5}$ and $4.3(\pm0.1) \times 10^{-4}$ s^{-1}, respectively (see ESI†). The reaction of ^{s}PhIO with 10 equivalents of PPh_3 was too rapid to monitor by this method; it was complete within 3 minutes of mixing. These data show that the rate of decay of ^{s}PhIO with thioanisole is at least an order of magnitude faster than for **1** and **2** under the same conditions and the rate with DHA is on the same order of magnitude as **1** and an order of magnitude faster than for **2** under similar conditions.

It has been previously shown for metal–porphyrin complexes that an equilibrium exists between metal iodosylarene adducts and the corresponding metal–oxo complexes.[13,17] This equilibrium can be shifted towards the metal iodosylarene adduct by addition of a sufficient excess of the iodoarene. In order to test whether the Co complexes presented here may reversibly form high-valent Co–oxo species, we tested the effect of added iodoarene on reaction rates. For complex **1**, an excess of ^{s}PhI (10 equivalents) was added and the self-decay monitored. Under these conditions, no change of the rate of self-decay was observed (see ESI†). The reactions of **2** and **3** with thioanisole or DHA were also investigated with the addition of excess iodoarene. In both cases, no inhibition was observed with additional ^{s}PhI. However, in the case of **2**, increased rates were observed and for **3**, a complex reaction occurred which produced unknown paramagnetic products in addition to the formation of **2** (see ESI†). While we do not have a concrete explanation for these observations, these experiments still oppose a simple reversible oxo formation pathway (see below).

Given a lack of reactivity studies that have been performed with discrete metal iodosyl- and iodoxyarene adducts, we sought to examine more carefully their C–H activation reactivity. As a mechanistic probe of C–H activation, KIEs for the reaction of **1–3** with DHA were measured. Due to the sluggish rates of reaction, we turned to a method reported in the literature for estimating KIE values using GCMS data from the relative ratio of the mass peaks of the H_2- and D_2-anthracene produced from the competition reaction of the oxidant with a 1 : 1 mixture of H_4- and D_4-DHA.[53] In these experiments, relatively large KIEs were observed for complexes **1**, **2**, and **3** (Table 1). With this method, it was difficult to precisely determine the KIE value for **1** because there was no increase in the amount of D_2-anthracene detected and instead a value is estimated with a lower bound of 12 using the variability in the instrument response for D_2-anthracene in the control mixture (see ESI† for more details). The KIE values for **2** and **3** could be determined more precisely at 14 and 9, respectively. The KIE for free ^{s}PhIO was also determined using this method and was found to have a lower bound of 3, which is consistent with the value reported for PhIO.[53] Additionally, controls were performed involving redox-innocent, diamagnetic Lewis acids to determine whether the higher KIE values for complexes **1–3** could be due to the influence of the paramagnetic Co ion. Oxidation reactions under the conditions described using ^{s}PhIO in the presence of either $Sc(OTf)_3$ or $NaBAr^{F}_{4}$ display a high selectivity for H_4-DHA to give KIE values of >66 and >11, respectively. These results suggest that a paramagnetic Lewis acid is not essential for the observation of large KIE values under these conditions. Furthermore, all of the observed KIEs are larger than that measured for free ^{s}PhIO, supporting the agency of metal-based intermediates in the observed reactivity as opposed to simple dissociation of ^{s}PhIO.

As a final set of experiments to explore the reactivity of the Co iodosyl- and iodoxyarene complexes, we examined the effect of a Lewis acid on their stability and reactivity. Recently, there have been several reports suggesting that in the oxidation of a Co complex with ^{s}PhIO, strong Lewis acids such as Sc^{3+} can stabilize high valent, $[Co–O–Sc]^{5+}$ moieties.[33,34] However, there has been some debate about the nature of these species,[54] prompting us to investigate the reactivity of our discrete adducts with Lewis acids. When complexes **2** and **3** were treated with excess $Sc(OTf)_3$, the only observed reaction was slow conversion to complex **5**, presumably from the coordination of OTf. When complex **1** was treated with excess $Sc(OTf)_3$ under the same conditions a mixture of products was obtained. We have been unable to purify a single species from this mixture, but we have crystallographically characterized a new asymmetric Co(II) complex which appears to be the major product by ^{1}H NMR analysis (**6**, see ESI†). Complex **6** shows a single Co center coordinated to two pyrazole arms from the Tp ligand, a free Ad,Me-pyrazole, and OTf with an outer sphere BAr^{F}_{4} ion. Notably, the mass spectrum of this solution did not show evidence of ligand oxidation that is typically observed in the self-decay of **1** (see ESI†). While there was no incorporation of Sc^{3+} or oxygen into the complex and we do not know the mechanism leading to ligand degradation, this new reaction product demonstrates an alternative pathway is operative for **1** when Sc^{3+} ions are added. These data do not allow us to definitively support or exclude the formation of transient, high-valent $[Co–O–Sc]^{5+}$ species.

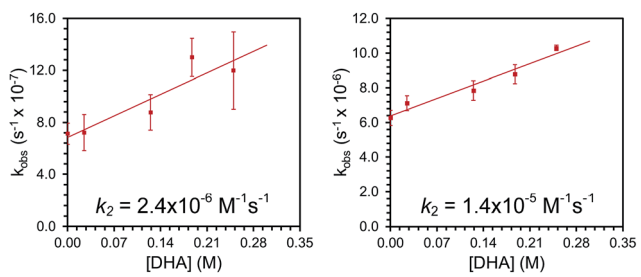

Fig. 2 Plots of observed rate constants for the reaction of **2** (left) and **3** (right) with varying concentrations of DHA to determine second order rate constants, k_2.

Discussion of possible mechanism

The key question that remains is the mode of oxidative activity for these complexes. As mentioned in the introduction, the

 This journal is © The Royal Society of Chemistry 2018

Open Access Article. Published on 23 April 2018. Downloaded on 2/20/2026 3:42:12 PM.
This article is licensed under a Creative Commons Attribution-NonCommercial 3.0 Unported Licence.

most common paradigm in the literature is a pathway involving adduct decomposition to form a high-valent oxo complex. In our case, we have considered three potential reaction pathways summarized in Fig. 3: (A) irreversible, rate-determining I–O bond scission to form a reactive, transient high-valent Co–oxo complex, (B) reversible I–O bond scission to form a transient Co–oxo complex or (C) direct oxidation of substrate by the Co iodosyl- or iodoxyarene adducts. We have ruled out a mechanism involving dissociation of the hypervalent iodine oxidants on the basis of the observed differences in rates of reactions and KIEs of free ^{s}PhIO and the Co adducts (see ESI†).

The data for complex **1** are consistent with a rate-determining, irreversible Co–oxo forming step (Fig. 3, pathway A). To be clear, we have no spectroscopic evidence for a Co–oxo species, but its potential involvement is proposed based on the observed reactivity and cannot be ruled out. The rate of decay of complex **1** was not inhibited by addition of excess ^{s}PhI, which argues against any equilibrium between **1** and a Co–oxo species as shown in pathway B of Fig. 3. If **1** were to follow pathway C, it is expected that the rate of decay would be dependent on substrate concentration. Instead, the rate of decay of **1** was not accelerated by external substrates, with the exception of phosphines. Furthermore, the decay of **1** results in a complicated mixture of paramagnetic products and some degree of ligand oxidation in the mixture can be inferred from the ESI-MS data. Finally, the large calculated KIE for **1** is comparable to other reported metal–oxo complexes.[55–57] These data taken together are consistent with the involvement of a Co–oxo intermediate in the case of **1**, but are certainly not conclusive on their own. At minimum the data support a distinct reactivity pathway for **1** compared with complexes **2** and **3**.

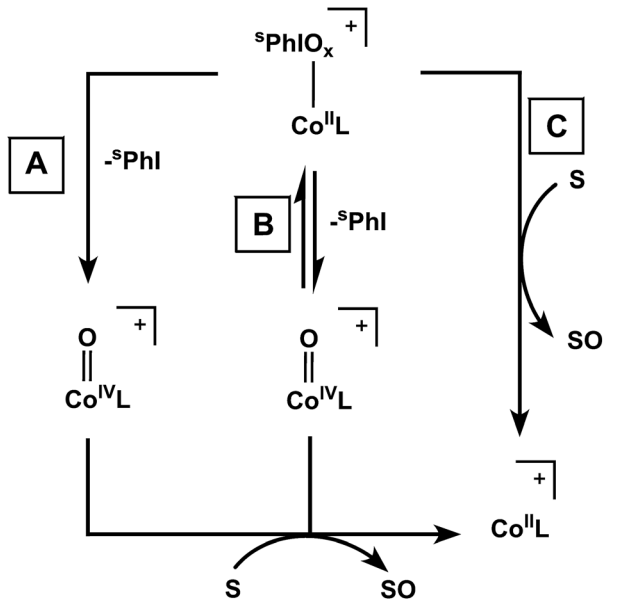

Fig. 3 Potential reaction pathways for Co–iodosyl- and iodoxyarene adducts **1–3** involving (A) irreversible Co–oxo formation, (B) reversible Co–oxo formation, or (C) direct substrate oxidation. Where L = Tp ligand, S = generic substrate molecule, and SO = oxidized substrate molecule.

For **2**, there is an observed substrate dependence on the rate of decay, suggesting I–O bond scission is not rate-limiting; this observation argues against pathway A. Furthermore, the reactivity of **2** is not inhibited by the addition of excess ^{s}PhI, which argues against a reversible oxo formation mechanism as would be observed in pathway B. These combined data support the direct agency of adduct **2** in the observed oxidative activity rather than decomposition into a Co–oxo complex (Fig. 3, pathway C). The observed large KIE for **2** also suggests that this adduct is directly involved in reactivity, as opposed to a dissociative pathway where free ^{s}PhIO acts as the active oxidant. Given that the electrochemistry for both the Ad and the ^{t}Bu systems shows similar electronic properties in both cases, the observed differences in reactivity between **1** and **2** are likely due to the differing steric profiles of these two systems.

The self-decay and observed substrate reactivity for **3** are similar to that of **2**, suggesting that a related mechanism may be operative. However, because formation of **2** is frequently observed in the reactivity of **3**, it is difficult to deconvolute relative contributions from these two species in certain experiments such as the KIE analysis and the inhibition of reactivity by added ^{s}PhI. These factors make it difficult to distinguish between pathways B and C, but the observed rate dependence on substrate concentration for **3** suggests that pathway A can be excluded.

Conclusions

Complexes **1** and **2** represent the first examples of isolable Co iodosylarene complexes and **3** represents the only example of a transition metal iodoxyarene complex to be thoroughly characterized. The studies herein demonstrate that these adducts display O-atom transfer reactivity and C–H bond activation with appropriate substrates. While the data are consistent with complex **1** reacting *via* transient oxo formation, complexes **2** and **3** appear to react directly as adducts. This series of complexes represents an unusual family of transition metal hypervalent iodine adducts and the detailed reactivity studies reported here further support the diverse reactivity that these species can exhibit. Notably, it must be underscored that these adduct species – which are frequently invoked only as intermediates – can be competent oxidants themselves in oxidative reactions.

Conflicts of interest

There are no conflicts of interest to declare.

Acknowledgements

ChemMatCARS Sector 15 is principally supported by the Divisions of Chemistry (CHE) and Materials Research (DMR), National Science Foundation (NSF), under Grant No. NSF/CHE-1346572. Use of the PILATUS3 X CdTe 1M detector is supported by the National Science Foundation under the grant number NSF/DMR-1531283. Use of the Advanced Photon Source, an Office of Science User Facility operated for the U.S. Department

Open Access Article. Published on 23 April 2018. Downloaded on 2/20/2026 3:42:12 PM. This article is licensed under a Creative Commons Attribution-NonCommercial 3.0 Unported Licence.

of Energy (DOE) Office of Science by Argonne National Laboratory, was supported by the U.S. DOE under Contract No. DE-AC02-06CH11357. We also thank Dr Yu-Sheng Chen for assistance with single crystal X-ray diffraction studies at beamline 15-ID-B. Work presented here was funded by the following sources: NSF CAREER award Grant No. 1654144, M. L. K. supported by the NSF Graduate Student Fellowship Grant No. DGE-1144082 and DGE-1746045, and the University of Chicago.

Notes and references

1 P. J. Stang and V. V. Zhdankin, *Chem. Rev.*, 1996, **96**, 1123–1178.
2 V. V. Zhdankin and P. J. Stang, *Chem. Rev.*, 2002, **102**, 2523–2584.
3 V. V. Zhdankin and P. J. Stang, *Chem. Rev.*, 2008, **108**, 5299–5358.
4 A. Yoshimura and V. V. Zhdankin, *Chem. Rev.*, 2016, **116**, 3328–3435.
5 J. T. Groves, T. E. Nemo and R. S. Myers, *J. Am. Chem. Soc.*, 1979, **101**, 1032–1033.
6 J. T. Groves, W. J. Kruper and R. C. Haushalter, *J. Am. Chem. Soc.*, 1980, **102**, 6375–6377.
7 W. J. Song, M. S. Seo, S. D. George, T. Ohta, R. Song, M.-J. Kang, T. Tosha, T. Kitagawa, E. I. Solomon and W. Nam, *J. Am. Chem. Soc.*, 2007, **129**, 1268–1277.
8 J. England, M. Martinho, E. R. Farquhar, J. R. Frisch, E. L. Bominaar, E. Münck and L. Que, *Angew. Chem., Int. Ed.*, 2009, **48**, 3622–3626.
9 A. I. Nguyen, R. G. Hadt, E. I. Solomon and T. D. Tilley, *Chem. Sci.*, 2014, **5**, 2874–2878.
10 J. D. Koola and J. K. Kochi, *J. Org. Chem.*, 1987, **52**, 4545–4553.
11 A. R. McDonald and L. Que, *Coord. Chem. Rev.*, 2013, **257**, 414–428.
12 J. P. Collman, A. S. Chien, T. A. Eberspacher and J. I. Brauman, *J. Am. Chem. Soc.*, 2000, **122**, 11098–11100.
13 W. Nam, S. K. Choi, M. H. Lim, J.-U. Rohde, I. Kim, J. Kim, C. Kim and L. Que, *Angew. Chem., Int. Ed.*, 2003, **42**, 109–111.
14 J. P. Collman, A. L. Zeng and J. I. Brauman, *Inorg. Chem.*, 2004, **43**, 2672–2679.
15 S. H. Wang, B. S. Mandimutsira, R. Todd, B. Ramdhanie, J. P. Fox and D. P. Goldberg, *J. Am. Chem. Soc.*, 2004, **126**, 18–19.
16 K. P. Bryliakov and E. P. Talsi, *Angew. Chem., Int. Ed.*, 2004, **43**, 5228–5230.
17 W. J. Song, Y. J. Sun, S. K. Choi and W. Nam, *Chem.–Eur. J.*, 2006, **12**, 130–137.
18 P. Leeladee and D. P. Goldberg, *Inorg. Chem.*, 2010, **49**, 3083–3085.
19 S. Hong, B. Wang, M. S. Seo, Y.-M. Lee, M. J. Kim, H. R. Kim, T. Ogura, R. Garcia-Serres, M. Clémancey, J.-M. Latour and W. Nam, *Angew. Chem., Int. Ed.*, 2014, **53**, 6388–6392.
20 B. Wang, Y.-M. Lee, M. S. Seo and W. Nam, *Angew. Chem., Int. Ed.*, 2015, **54**, 11740–11744.
21 J. D. Protasiewicz, in *Hypervalent Iodine Chemistry*, ed. T. Wirth, Springer, Cham, 2015, pp. 263–288.
22 Y. Kang, X.-X. Li, K.-B. Cho, W. Sun, C. Xia, W. Nam and Y. Wang, *J. Am. Chem. Soc.*, 2017, **139**, 7444–7447.
23 M. J. Zdilla and M. M. Abu-Omar, *J. Am. Chem. Soc.*, 2006, **128**, 16971–16979.
24 M. M. Abu-Omar, *Dalton Trans.*, 2011, **40**, 3435–34444.
25 A. Lennartson and C. J. McKenzie, *Angew. Chem., Int. Ed.*, 2012, **51**, 6767–6770.
26 D. P. de Sousa, C. Wegeberg, M. S. Vad, S. Mørup, C. Frandsen, W. A. Donald and C. J. McKenzie, *Chem.–Eur. J.*, 2016, **22**, 3810–3820.
27 C. Wang, T. Kurahashi and H. Fujii, *Angew. Chem., Int. Ed.*, 2012, **51**, 7809–7811.
28 C. Wang, T. Kurahashi, K. Inomata, M. Hada and H. Fujii, *Inorg. Chem.*, 2013, **52**, 9557–9566.
29 C. R. Turlington, J. Morris, P. S. White, W. W. Brennessel, W. D. Jones, M. Brookhart and J. L. Templeton, *Organometallics*, 2014, **33**, 4442–4448.
30 K.-C. Au-Yeung, Y.-M. So, G.-C. Wang, H. H.-Y. Sung, I. D. Williams and W.-H. Leung, *Dalton Trans.*, 2016, **45**, 5434–5438.
31 G. de Ruiter, K. M. Carsch, S. Gul, R. Chatterjee, N. B. Thompson, M. K. Takase, J. Yano and T. Agapie, *Angew. Chem., Int. Ed.*, 2017, **56**, 4772–4776.
32 B. Wang, Y.-M. Lee, W.-Y. Tcho, S. Tussupbayev, S.-T. Kim, Y. Kim, M. S. Seo, K.-B. Cho, Y. Dede, B. C. Keegan, T. Ogura, S. H. Kim, T. Ohta, M.-H. Baik, K. Ray, J. Shearer and W. Nam, *Nat. Commun.*, 2017, **8**, 14839.
33 S. Hong, F. F. Pfaff, E. Kwon, Y. Wang, M.-S. Seo, E. Bill, K. Ray and W. Nam, *Angew. Chem., Int. Ed.*, 2014, **53**, 10403–10407.
34 F. F. Pfaff, S. Kundu, M. Risch, S. Pandian, F. Heims, I. Pryjomska-Ray, P. Haack, R. Metzinger, E. Bill, H. Dau, P. Comba and K. Ray, *Angew. Chem., Int. Ed.*, 2011, **50**, 1711–1715.
35 E. F. Caldin, *Chem. Rev.*, 1969, **69**, 135–156.
36 Z. Cong, H. Kinemuchi, T. Kurahashi and H. Fujii, *Inorg. Chem.*, 2014, **53**, 10632–10641.
37 D. Mandal, D. Mallick and S. Shaik, *Acc. Chem. Res.*, 2018, **51**, 107–117.
38 J. M. Mayer, *Acc. Chem. Res.*, 2011, **44**, 36–46.
39 D. Macikenas, E. Skrzypczak-Jankun and J. D. Protasiewicz, *J. Am. Chem. Soc.*, 1999, **121**, 7164–7165.
40 F. Song, C. Wang, J. M. Falkowski, L. Ma and W. Lin, *J. Am. Chem. Soc.*, 2010, **132**, 15390–15398.
41 D. Macikenas, E. Skrzypczak-Jankun and J. D. Protasiewicz, *Angew. Chem., Int. Ed.*, 2000, **39**, 2007–2010.
42 A. McSkimming and W. H. Harman, *J. Am. Chem. Soc.*, 2015, **137**, 8940–8943.
43 *Inorganic Syntheses*, ed. R. J. Angelici, John Wiley & Sons, Inc., Hoboken, NJ, USA, 1990, vol. 28.
44 C. Goldsmith, R. Jonas and T. Stack, *J. Am. Chem. Soc.*, 2002, **124**, 83–96.
45 N. Chakrabarti, W. Sattler and G. Parkin, *Polyhedron*, 2013, **58**, 235–246.
46 I. B. Gorrell and G. Parkin, *Inorg. Chem.*, 1990, **29**, 2452–2456.
47 S. Thyagarajan, C. D. Incarvito, A. L. Rheingold and K. H. Theopold, *Inorg. Chim. Acta*, 2003, **345**, 333–339.

 This journal is © The Royal Society of Chemistry 2018

Open Access Article. Published on 23 April 2018. Downloaded on 2/20/2026 3:42:12 PM.
This article is licensed under a Creative Commons Attribution-NonCommercial 3.0 Unported Licence.

48 J. D. Jewson, L. M. Liable-Sands, G. P. A. Yap, A. L. Rheingold and K. H. Theopold, *Organometallics*, 1999, **18**, 300–305.
49 J. L. Detrich, R. Konečný, W. M. Vetter, D. Doren, A. L. Rheingold and K. H. Theopold, *J. Am. Chem. Soc.*, 1996, **118**, 1703–1712.
50 S. Thyagarajan, C. D. Incarvito, A. L. Rheingold and K. H. Theopold, *Chem. Commun.*, 2001, 2198–2199.
51 J. W. Egan, B. S. Haggerty, A. L. Rheingold, S. C. Sendlinger and K. H. Theopold, *J. Am. Chem. Soc.*, 1990, **112**, 2445–2446.
52 C. R. Groom, I. J. Bruno, M. P. Lightfoot and S. C. Ward, *Acta Crystallogr., Sect. B: Struct. Sci., Cryst. Eng. Mater.*, 2016, **72**, 171–179.
53 S. J. Kim, R. Latifi, H. Y. Kang, W. Nam and S. P. de Visser, *Chem. Commun.*, 2009, **13**, 1562.
54 D. C. Lacy, Y. J. Park, J. W. Ziller, J. Yano and A. S. Borovik, *J. Am. Chem. Soc.*, 2012, **134**, 17526–17535.
55 A. Gunay and K. H. Theopold, *Chem. Rev.*, 2010, **110**, 1060–1081.
56 L. Q. Shen, S. Kundu, T. J. Collins and E. L. Bominaar, *Inorg. Chem.*, 2017, **56**, 4347–4356.
57 S. N. Dhuri, K.-B. Cho, Y.-M. Lee, S. Y. Shin, J. H. Kim, D. Mandal, S. Shaik and W. Nam, *J. Am. Chem. Soc.*, 2015, **137**, 8623–8632.